

A new Cu Schiff base complex with histidine and glutaraldehyde immobilized on modified iron oxide nanoparticles as a recyclable catalyst for the oxidative homocoupling of terminal alkynes

Faezeh Farzaneh¹ · Elnaz Rashtizadeh¹

Received: 25 July 2015 / Accepted: 19 February 2016
© Iranian Chemical Society 2016

Abstract The novel functionalized $\text{Fe}_3\text{O}_4@\text{SiO}_2@\text{APTMS}@Glu\text{-His}@Cu$ complex was prepared from modification of iron oxide nanomagnet particles with (3-aminopropyl) trimethoxysilane (APTMS) and glutaraldehyde–histidine Schiff base followed by complexation with Cu(I) salt. Characterization of this complex was carried out by means of FTIR, XRD, SEM, TEM and VSM techniques. The complex was found to successfully catalyze the oxidative homocoupling of phenylacetylene, 4-*tert*-butylphenylacetylene, 1-ethynyl-4-fluorobenzene and pent-1-yn-3-ol with 67–100 % conversions and 95–100 % selectivities. Magnetic recovery and recycling of the catalyst without significant decrease in activity is described in this presentation.

Keywords Modified magnetic nanoparticles · Oxidative homocoupling · Terminal alkynes · Schiff base copper complex

Introduction

The homocoupling of terminal alkynes to 1,3-diynes is an important carbon–carbon bond-formation reaction. 1,3-Diynes are widespread in many natural products

[1–3], pharmaceuticals [4, 5], and bioactive compounds [6] with anti-inflammatory [7], antifungal [8], anti-HIV, antibacterial, or antitumor activities [9]. Acetylenic couplings cover a large area of scientific interests for the synthesis of key structural motifs in linearly π -conjugated acetylenic oligomers and polymers [10], macrocyclic annulene [11], agrochemicals, organic conductors, supramolecular switches, carbon-rich materials [12, 13], liquid crystals, molecular wires and non-linear optic materials [14]. Therefore, much attention has been made to the development of efficient synthetic procedures for the diyne derivatives. The Cu-catalysis systems have widely been used for homocoupling reactions (first discovered by Glaser in 1869) [15]. After the seminal paper published by Glaser, many efforts have been devoted toward the development of milder and more environmentally friendly protocols for the homocoupling of terminal alkynes. In this regard, a number of catalysis systems have been developed. Palladium and copper salts are efficient and mild catalysis systems for the homocoupling of terminal alkynes [16–24]. However, palladium catalysts are expensive and air-sensitive and either phosphine or amine ligands are usually required.

Whereas most homocoupling reactions were initially carried out by homogeneous catalysis systems, the easy separation and privilege of recycling of the heterogeneous catalysts after the reaction workup increases the feasibility of the reaction even in large scale fine-chemical applications. Utilization of heterogeneous catalysis system generally minimizes the contamination of organic reaction mixtures by the catalyst with along with significant advantage in terms of time demanding purification procedures. Supported copper on inorganic supports such as silica [25], Al-MCM-41 [26], zeolites [27], titanium oxide [28, 29] and SBA-15 [30], are some representative examples of

Electronic supplementary material The online version of this article (doi:10.1007/s13738-016-0829-7) contains supplementary material, which is available to authorized users.

✉ Faezeh Farzaneh
faezeh_farzaneh@yahoo.com; farzaneh@alzahra.ac.ir

¹ Department of Chemistry, Faculty of Physics and Chemistry, Alzahra University, P. O. Box 1993891176, Vanak, Tehran, Iran

heterogeneous catalytic systems effectively applied to the homocoupling of terminal alkynes.

Another set of heterogeneous catalytic systems are nano-magnetic catalysts due to easily separation from the reaction medium using an external magnetic field, which avoids loss of catalyst and increases its reusability and improve its recovery rate during separation process in comparison to filtration or centrifugation. Additionally, nano-catalyst with large specific surface area and high catalytic activity also exhibits good catalytic property [31]. Whereas magnetic or nano-magnetic particles have been widely applied as catalyst in many reactions such as hydrogenation [32], Suzuki–Miyaura reaction [33], olefin metathesis [34] and oxidation reactions [35], but there are only a few reports on using these materials as catalyst for oxidative homocoupling of terminal alkynes [36].

In this work, attempts has been made to functionalize the magnetite nanoparticles with 3-aminopropyl trimethoxysilane and then incorporate a copper Schiff base complex to obtain a heterogeneous copper catalyst for the homocoupling of terminal alkynes.

Experimental

Materials

All materials were of commercial reagent grade and used without further purification. Copper(I) iodide, Copper (II) acetate, phenylacetylene, sodium carbonate, 1-ethynyl-4-fluorobenzene, 4-tertbutylphenylacetylene, sodium chloride, ethylenediamine, 3-aminopropyltrimethoxysilane (APTMS), glycerol, iron(II) chloride ($\text{FeCl}_2 \cdot 4\text{H}_2\text{O}$), iron(III) chloride ($\text{FeCl}_3 \cdot 6\text{H}_2\text{O}$), ammonium hydroxide [25 % (w/w)], ethyl propiolate, 1-pentyn-3-ol, 1,4-diazabicyclo[2.2.2]octane (DABCO), sodium silicate, hydrochloric acid, methanol, ethanol, benzonitrile, glutaraldehyde, L-histidine, acetonitrile and dimethylformamide were purchased from Merck Chemical Company.

Characterization

C–C homocoupling products were analyzed by GC and GC-Mass using Agilent 6890 series with a FID detector, HP-5, 5 % phenylmethylsiloxane capillary and helium as carrier gas and Agilent 5973 network, mass selective detector, HP-5 MS 6989 network GC system. The X-ray diffractions (XRD) patterns of samples were recorded on a Philips PW1800 diffractometer using monochromatic nickel-filtered Cu K_α radiation ($k = 0.15405 \text{ nm}$). The X-ray generator was run at 40 kV and 30 mA and the diffractograms were recorded in the 2 h range of 4° – 90° . The phases were identified using the powder diffraction file (PDF) database (JCPDS, International Centre for Diffraction Data).

Magnetic measurements were carried out using a Quantum Design vibrating sample magnetometer (VSM) at room temperature in an applied magnetic field sweeping from -15 to 15 kOe . Structural examination of the catalyst by scanning electron microscope (SEM) was performed on a LEO 1455VP operating at an accelerated voltage of 20 kV and Transmission electron microscopy (TEM) images were taken by Zeiss-EM10C-100 KV. FTIR spectra of the samples were collected on a Bruker (Tensor 27) instrument in the range of 4000 – 400 cm^{-1} (5 mg sample with 100 mg KBr) under the atmospheric condition. The chemical analysis was carried out with an atomic absorption Chermo double beam instrument.

Preparation of amine-functionalized magnetic silica nanoparticles

Fe_3O_4 magnetic nanoparticles (MNPs), prepared according to the previously reported method were coated with silica [37]. A solution of $\text{Fe}_3\text{O}_4 @ \text{SiO}_2$ (0.2 g) was then dispersed in aqueous ethanol (20 %, 50 mL). APTMS (0.3 mL) was added dropwise by ultrasonic treatment and the mixture stirred for several hours. The brown modified MNPs solid was subsequently separated and neutralized by washing with HCl (0.1 M) for several times.

Preparation of Schiff base (Glu-His)

An aqueous solution of L-histidine (0.155 g, 0.1 M in deionized water) was added to glutaraldehyde (0.188 mL, 0.1 M in 10 mL deionized water). The solution was then heated at 45°C for 2 h. Observation of the solution color change from transparent to light yellow after 30 min indicated the completion of the reaction and formation of the product (denoted as Glu-His) [38].

Preparation of $\text{Fe}_3\text{O}_4 @ \text{SiO}_2 @ \text{APTMS}$

Immobilized Glu-His was obtained by stirring the $\text{Fe}_3\text{O}_4 @ \text{SiO}_2 @ \text{APTMS}$ (1.0 g) with Glu-His (10 mL) at 80°C for 2 h. It was assumed that the Schiff base between $\text{Fe}_3\text{O}_4 @ \text{SiO}_2 @ \text{APTMS}$ amino group and free aldehyde of the Glu-His has been generated in this reaction [38]. The brown solid product separated by means of an external magnet was washed with deionized water for several times.

Preparation of $\text{Fe}_3\text{O}_4 @ \text{SiO}_2 @ \text{APTMS} @ \text{Glu-His} @ \text{Cu}$ complex

$\text{Fe}_3\text{O}_4 @ \text{SiO}_2 @ \text{APTMS} @ \text{Glu-His}$ (1.0 g) was added to a solution of CuI (0.06 M in water) and the resultant mixture stirred over 8 h at 80°C . The solid product was then separated, washed with water and acetone and dried in air.

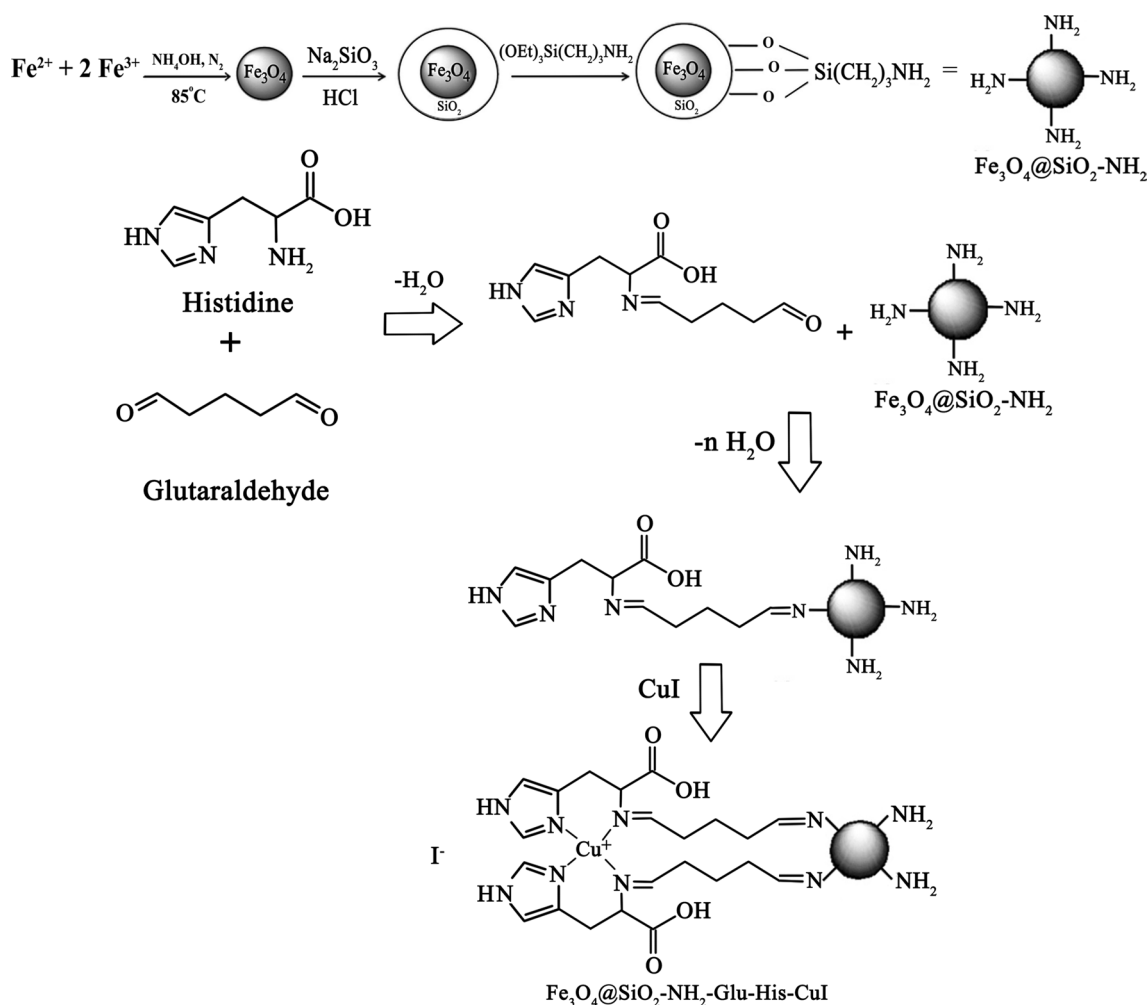
Catalytic reactions

The catalytic reactions were carried out in a round bottom flask equipped with a magnetic stirrer and a water-cooled condenser under O₂ atmosphere. Typically, a desired amount of catalyst, substrate (1.0 mmol), solvent (5 mL) and Na₂CO₃ (0.211 g, 2.0 mmol) were added to the reaction flask and the mixture heated at reflux within the desired time. The progress of reaction was monitored by TLC and GC, until the complete conversion of starting material. Separation of the catalyst was carried out by means of an external magnet and the solution subjected to GC and GC mass for analysis. After the conventional work up, the residue was purified using column chromatography (petroleum ether/ethylacetate). The products were confirmed by the comparison of their GC retention time, GC mass, with those of authentic data (Figure S1-5, see supplementary) [22, 24].

Results and discussion

Catalyst characterization

Fe₃O₄@SiO₂@APTMS@Glu-His@Cu complex designated as compound **1** was prepared according to the procedure presented in Scheme 1. MNPs were initially prepared by precipitation of iron(II) and iron(III) ions in a basic solution. Subsequently, silica was coated on Fe₃O₄ to form Fe₃O₄@SiO₂ core-shell particles using sodium silicate in acidic solution to prevent the aggregation and increasing the stability of Fe₃O₄ nanoparticles in a harsh liquid environment. The modification of magnetic nanoparticles surface is generally carried out by functionalization with desired organic groups [38, 39]. Therefore, after the surface functionalization with APTMS, Glu-His Schiff base was immobilized followed



Scheme 1 Preparation steps of Fe₃O₄@SiO₂@APTMS@Glu-His@Cu complex magnetic nanoparticles

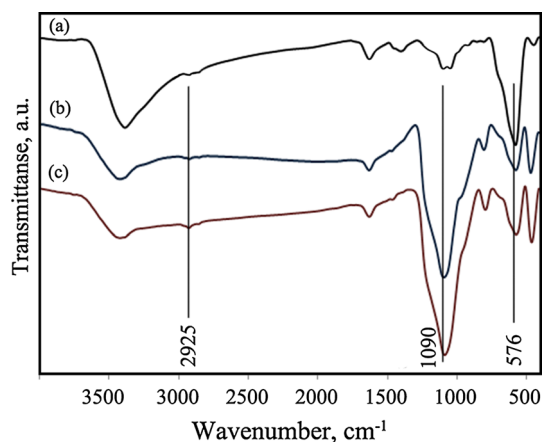


Fig. 1 The FTIR spectra of (a) Fe_3O_4 , (b) $\text{Fe}_3\text{O}_4@SiO_2$, (c) $\text{Fe}_3\text{O}_4@SiO_2@APTMS$

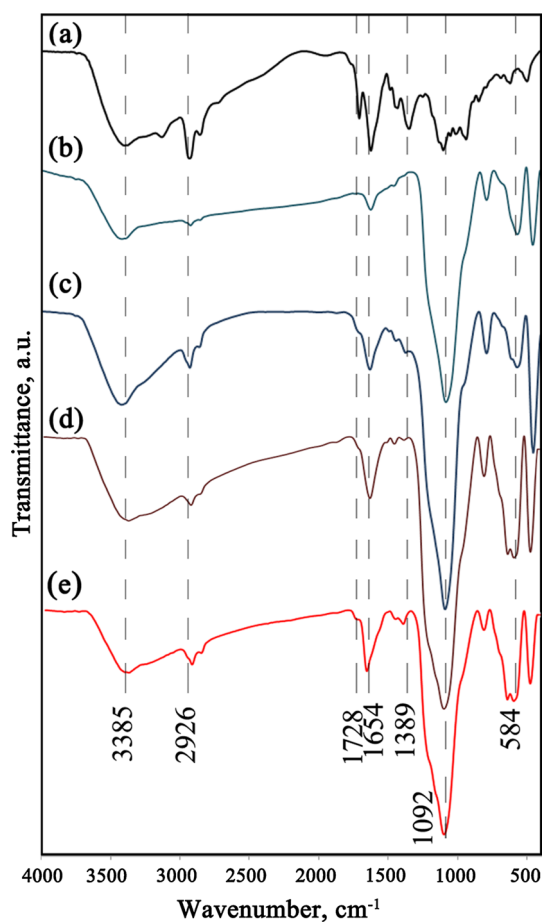


Fig. 2 The FTIR spectra of (a) Glu-His, (b) $\text{Fe}_3\text{O}_4@SiO_2@APTMS$, (c) $\text{Fe}_3\text{O}_4@SiO_2@APTMS@Glu-His$, (d) $\text{Fe}_3\text{O}_4@SiO_2@APTMS@Glu-His@Cu$ complex before using and (e) after using as catalyst

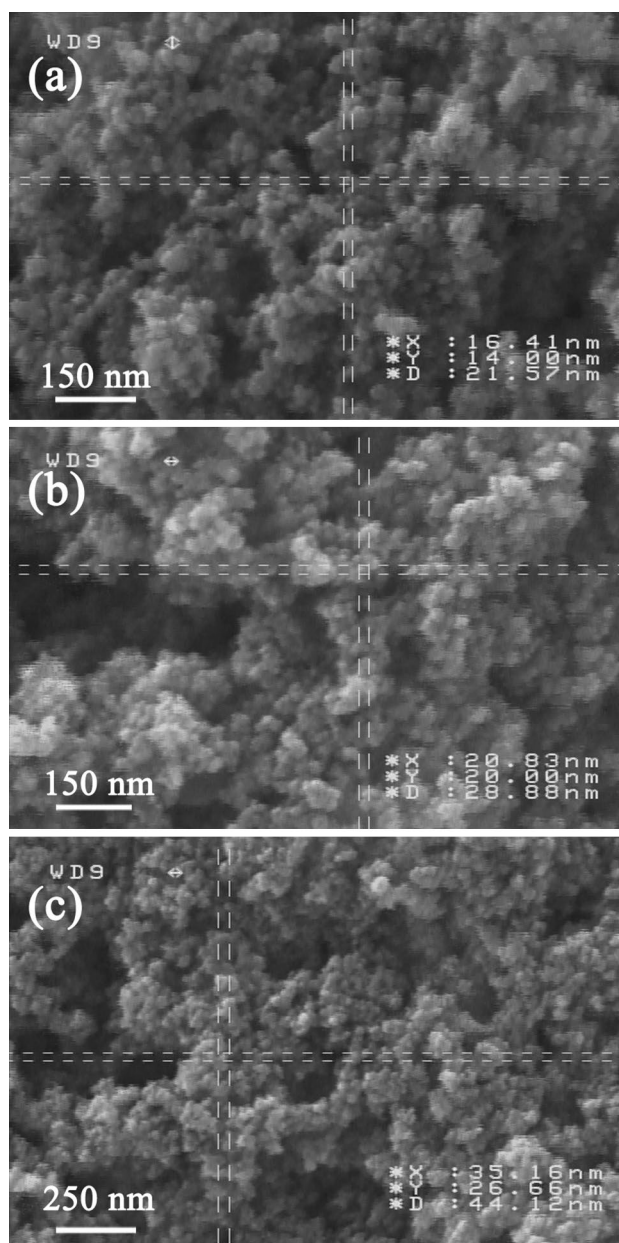


Fig. 3 The SEM images of a Fe_3O_4 , b $\text{Fe}_3\text{O}_4@SiO_2@APTMS$ and c $\text{Fe}_3\text{O}_4@SiO_2@APTMS@Glu-His@Cu$ complex

by complexation with CuI to afford the desired $\text{Fe}_3\text{O}_4@SiO_2@APTMS@Glu-His@Cu$ complex nanoparticles (see, Scheme 1).

The FT-IR spectra of Fe_3O_4 , $\text{Fe}_3\text{O}_4@SiO_2$ and $\text{Fe}_3\text{O}_4@SiO_2@APTMS$ are presented in Fig. 1a–c, respectively. As indicated in Fig. 1a, the bands appearing at 448 and 579 cm^{-1} are attributed to the Fe–O vibrations. In addition, observation of the bands displaying at 571 and 1090 cm^{-1}

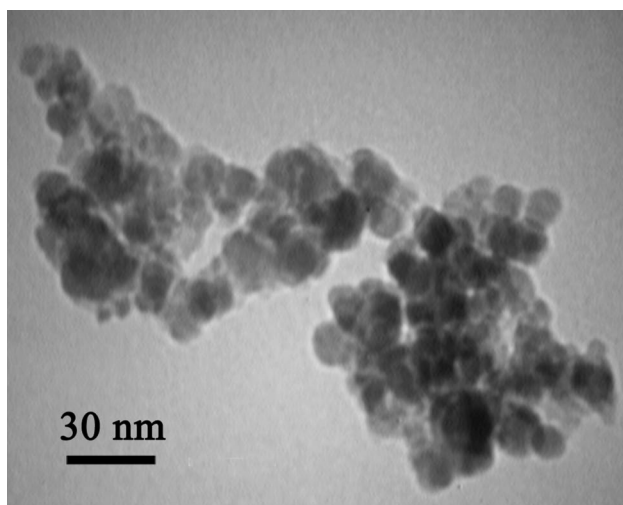


Fig. 4 The TEM image of $\text{Fe}_3\text{O}_4@SiO_2@APTMS@Glu-His@Cu$ complex

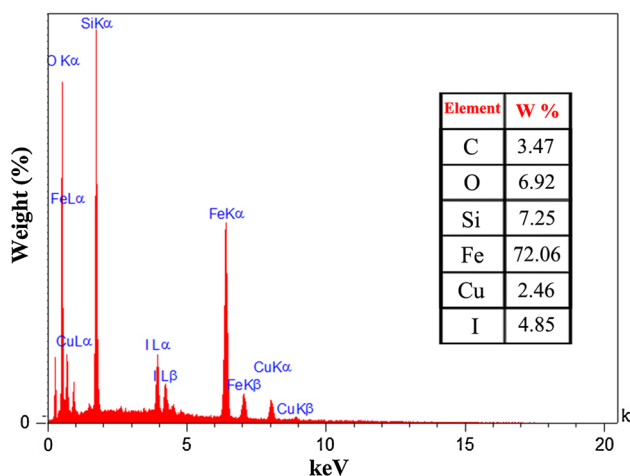


Fig. 5 The EDS of $\text{Fe}_3\text{O}_4@SiO_2@APTMS@Glu-His@Cu$ complex

due to the Fe–O and Si–O vibrations demonstrate the existence of Fe_3O_4 and SiO_2 components. After the functionalizing with APTMS, two obvious bands appearing at 2855 and 2925 cm^{-1} are associated with C–H stretching vibrations. This is in accordance with the predicted structure of $\text{Fe}_3\text{O}_4@SiO_2@APTMS$ (Fig. 1c) [40].

The FTIR spectra of Schiff base Glu-His, $\text{Fe}_3\text{O}_4@SiO_2@APTMS$, $\text{Fe}_3\text{O}_4@SiO_2@APTMS@Glu-His$, $\text{Fe}_3\text{O}_4@SiO_2@APTMS@Glu-His@Cu$ complex before and after using as catalyst are shown in Fig. 2a–c, respectively. The spectrum of the Schiff base Glu-His (Fig. 2a) shows a band at the region 1360 cm^{-1} due to the C–N vibrations. Moreover, whereas the rather strong band displaying at 1635 cm^{-1} is assigned to the C=N stretching vibration, that appearing at 1728 cm^{-1} is attributed to the C=O stretching vibration

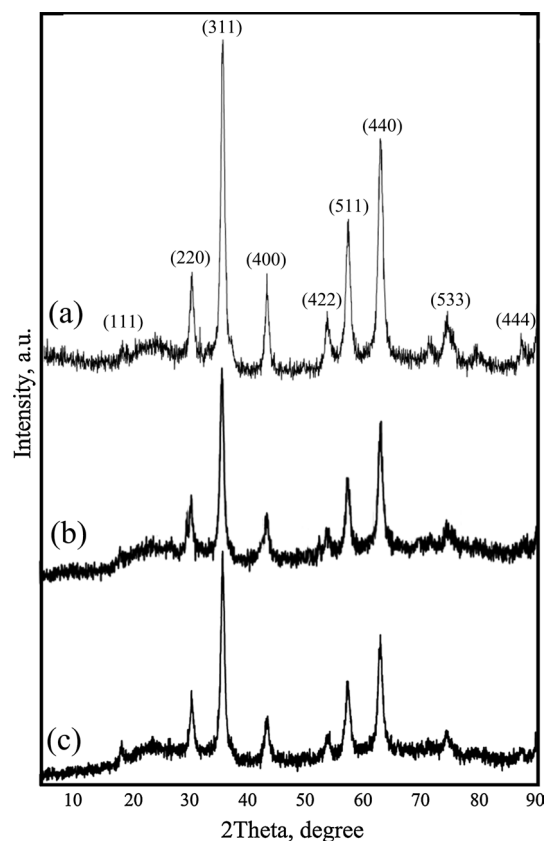


Fig. 6 XRD pattern of (a) $\text{Fe}_3\text{O}_4@SiO_2@APTMS$, (b) $\text{Fe}_3\text{O}_4@SiO_2@APTMS@Glu-His@Cu$ complex before using and (c) after using as catalyst

of aldehyde group. Compared to the FTIR spectrum of $\text{Fe}_3\text{O}_4@SiO_2@APTMS$ (Fig. 2b), several changes can be observed in all the frequency ranges in the spectrum of the immobilized Schiff base (Fig. 2c). For example, increasing the intensity of C=N and C–H stretching.

Vibrations observed respectively at 1637 and 2865 and 2940 cm^{-1} indicates the Glu-His group bonded to $\text{Fe}_3\text{O}_4@SiO_2@APTMS$. Moreover, whereas the C=N stretching vibrations of the Glu-His in $\text{Fe}_3\text{O}_4@SiO_2@APTMS@Glu-His$ is traditionally appeared at 1637 cm^{-1} , shifting to a lower wave number at 1630 cm^{-1} by approximately 7 cm^{-1} confirms the coordination of the Schiff base nitrogen atom to the metal ion (Fig. 2d). A broad band observed in the range of 2400–3400 cm^{-1} due to the histidine OH stretching of carboxyl group indicates that no coordination to the metal ion has occurred [38, 41].

Based on the SEM results (Fig. 3a–c), the change in the particle size after immobilization of Glu-His and Cu complex on modified MNPs is considerable (Fig. 3b, c). Moreover, the particles size was found to be about 15–35 nm based on the TEM results of $\text{Fe}_3\text{O}_4@SiO_2@APTMS@Glu-His@Cu$ complex indicated in Fig. 4. The EDS of

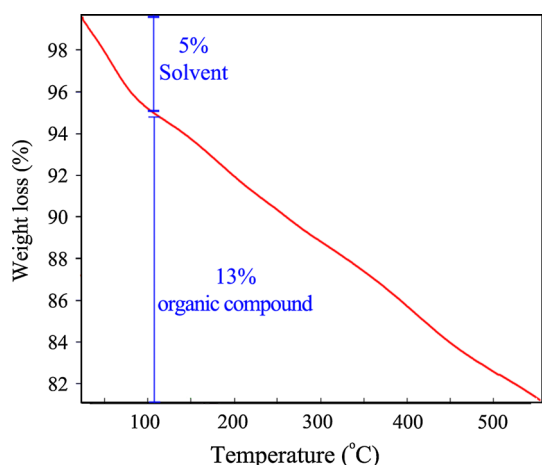


Fig. 7 The TGA of Fe₃O₄@SiO₂@APTMS@Glu-His@Cu complex

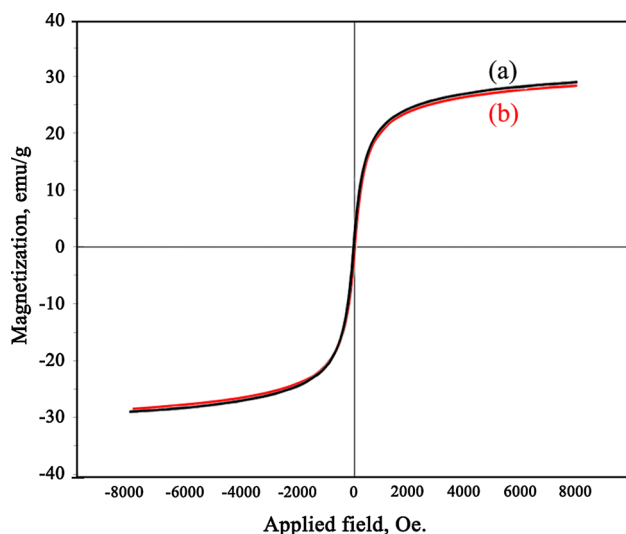


Fig. 8 Magnetization curves of (a) Fe₃O₄@SiO₂@APTMS@Glu-His@Cu complex before and (b) after using as catalyst

Fe₃O₄@SiO₂@APTMS@Glu-His@Cu complex is shown in Fig. 5. The results confirm the presence of Cu, Si, Fe, I and C in the sample.

The XRD patterns of the prepared Fe₃O₄@SiO₂@APTMS, Fe₃O₄@SiO₂@APTMS@Glu-His@Cu complex before and after using as catalyst are shown in Fig. 6a–c. The diffraction peaks with *d* values at 4.90, 2.95, 2.52, 2.08, 1.70, 1.60, 1.48, 1.27 and 1.11 observed for Fe₃O₄@SiO₂@APTMS nanoparticles are related to the (111), (220), (311), (400), (422), (511), (440), (533), and (444) planes (Fig. 6a). These results are similar to those of the standard JCPDS card No. 1-1111 exhibiting the iron oxide

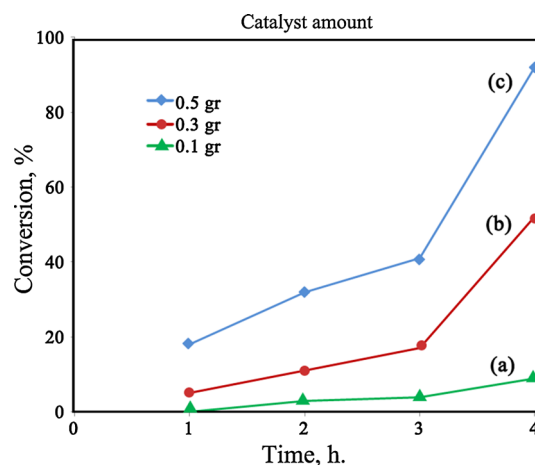


Fig. 9 Effect of the amount of compound 1 as catalyst and time on conversion at 100 °C under O₂ atmosphere, in the presence of sodium carbonate as base and DMF as solvent

characteristic peaks with cubic structure. The similar set of characteristic peaks also observed for Fe₃O₄@SiO₂@APTMS@Glu-His@Cu complex indicate the stability of the Fe₃O₄ nanoparticle crystalline phase during silica coating and surface amino-functionalization.

Thermal decomposition of Fe₃O₄@SiO₂@APTMS@Glu-His@Cu complex was studied. As seen in this Fig. 7, the first and second weight lossings up to 110 and 550 °C should be due to the removal of water and organic phase decompositions, respectively.

The magnetic properties of the prepared catalyst containing a magnetite component were studied by a VSM at 300 K. The magnetization curve of Fe₃O₄@SiO₂@APTMS@Glu-His@Cu complex before and after using as catalyst are shown in Fig. 8a, b. Since both remanence and coercivity are zero and no hysteresis is observed, it can be concluded that such nanospheres are superparamagnetic [37]. The saturation magnetization values for these catalysts were determined to be 30 emu/g (Fig. 8a, b).

Catalytic activity

Fe₃O₄@SiO₂@APTMS@Glu-His@Cu complex (1) was used as catalyst for the alkyne–alkyne homocoupling reaction and phenylacetylene was used as the representative substrate. To see the effect of catalyst amount and time on the product distribution, reaction times of 1, 2, 3 and 4 h were examined in the presence of 0.1–0.5 g of catalyst. The results indicated in Fig. 9 shows that by increasing the catalyst amount from 0.1 to 0.5 g, reaction conversion increases from 9 to 92 % during 4 h.

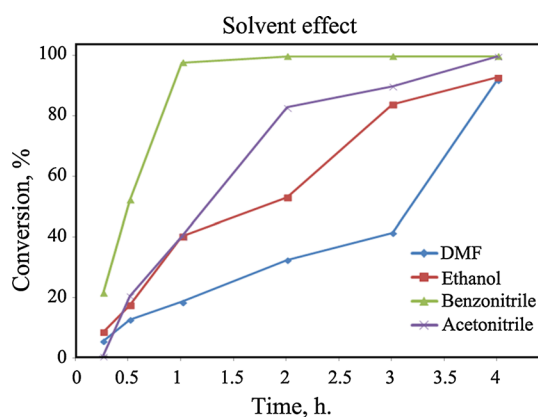


Fig. 10 Effect of solvent with compound **1** as catalyst, at reaction temperature 100 °C under O₂ atmosphere, in the presence of sodium carbonate as base

The effect of time with different solvents such as ethanol, acetonitrile, benzonitrile, and DMF on homocoupling reaction of phenylacetylene catalyzed by Fe₃O₄@SiO₂@APTMS@Glu-His@Cu complex (**1**) is presented in Fig. 10. As seen in Fig. 10, the best conversion was achieved in benzonitrile within 2 h. Hence, benzonitrile was selected as the reaction solvent for subsequent reactions.

Investigation of the effect of base on the model reaction revealed that whereas DABCO, sodium carbonate and sodium acetate afforded excellent yields (97–100 %), reaction was rather inefficient using triethylamine (32 %) (Fig. 11).

In the next step, 4-*tert*-butylphenylacetylene, 4-fluorophenylacetylene, ethyl propionate and pent-1-yn-3-ol were then examined for homocoupling reactions using benzonitrile as solvent and O₂ as oxidant in the presence of 0.5 g of Fe₃O₄@SiO₂@APTMS@Glu-His@Cu complex (**1**) as catalyst and sodium carbonate as base (Table 1). The products were characterized by comparison of the GC and GC–MS spectra with those of the authentic samples (see supplementary).

To test the reusability of the catalyst, compound **1** was recovered by external magnet from reaction mixture after completion of the first run and the catalyst was investigated in another run by addition of fresh phenylacetylene and benzonitrile similar to the initial reaction. A small decrease in catalyst activity from 98 % to the 91 % clearly revealed the reusability of the prepared catalyst (Fig. 12).

The stability of the magnetically recovered Fe₃O₄@SiO₂@APTMS@Glu-His@Cu complex (**1**) was also

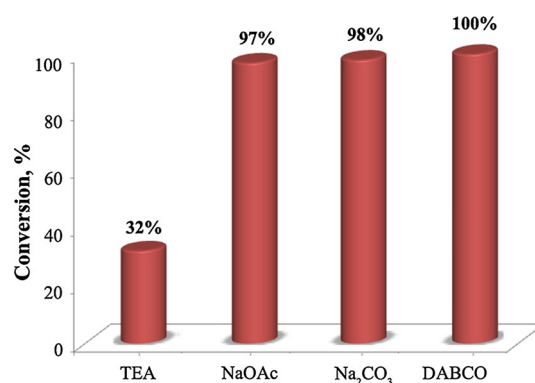


Fig. 11 Effect of different base with compound **1** as catalyst, at reaction temperature 100 °C under O₂ atmosphere

studied by recycling the recovering catalyst and determination of the copper content using atomic absorption spectroscopy. The copper content of the fresh and used catalysts were determined to be 2.41 and 2.38 %, respectively.

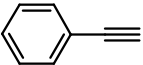
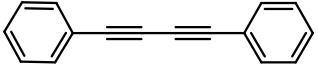
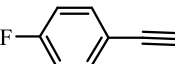
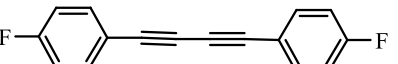
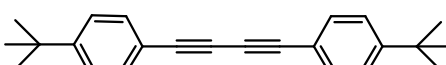
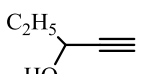
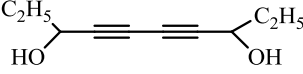
To further investigate the heterogeneous character of catalyst, compound **1** was recovered by external magnet from reaction mixture after 30 min. The reaction was then allowed to continue in the absence of catalyst. The observation of no additional conversion clearly indicated the heterogeneous character of the catalyst. On the other hand, the similarity of the FTIR, XRD and VSM patterns of Fe₃O₄@SiO₂@APTMS@Glu-His@Cu complex before and after using as catalyst shown respectively in Figs. 2e, 4c, and 5b also supported the catalyst stability.

As outlined in Scheme 2, we have formulated a working mechanism for the copper-catalyzed homocoupling of terminal alkynes based on the proposed mechanism of the previous reports and our results [42].

The initially generated Cu(I)-acetylide intermediate **I** from the base-catalyzed reaction of phenylacetylene with copper site of **1** (path a) is dimerized, affording **II** (path b). Subsequent intramolecular rearrangement with concomitant reduction of Cu(I) to Cu(0) together with homocoupling reaction affords intermediate **III** (path c). The product 1,3-diyne and regeneration of catalyst **1** occur via oxidation of **III** with O₂ (path d). To obtain further insight into the reaction mechanism, the homocoupling reaction of phenylacetylene was carried out in the presence of diphenylamine as a radical scavenger. The involvement of a free-radical pathway and implication of alkynyl radical in the reaction mechanism was ruled out since no considerable change in reaction rate and product selectivity was observed in the presence of diphenylamine as a radical scavenger.

Table 1 Results obtained for the homocoupling reaction of different monosubstituted terminal alkynes catalyzed by $\text{Fe}_3\text{O}_4@\text{SiO}_2@\text{APTMS}@$ Glu-His@Cu complex

$$2 \text{ R}-\text{C}\equiv\text{C}-\text{H} \xrightarrow[\text{sodium carbonate, benzonitrile, } 100^\circ\text{C, O}_2]{\text{Fe}_3\text{O}_4@\text{SiO}_2-\text{NH}_2-\text{Glu-His-Cu-complex}} \text{R}-\text{C}\equiv\text{C}-\text{C}\equiv\text{C}-\text{R}$$

Substrate	Product	Time (min)	Conversion (%)	Selectivity (%)
		30 60	52 100	100 100
		30 60	61 100	100 100
		30 60	74 100	100 100
$\text{EtO}_2\text{C}-\text{C}\equiv\text{C}-\text{H}$	$\text{EtO}_2\text{C}-\text{C}\equiv\text{C}-\text{C}\equiv\text{C}-\text{CO}_2\text{Et}$	30 60	63 100	100 100
		30 60	70 100	100 100

Reaction conditions: substrate (1 mmol), catalyst (0.5 g), sodium carbonate (2 mmol), benzonitrile (5 mL) at 100 °C under O_2 atmosphere

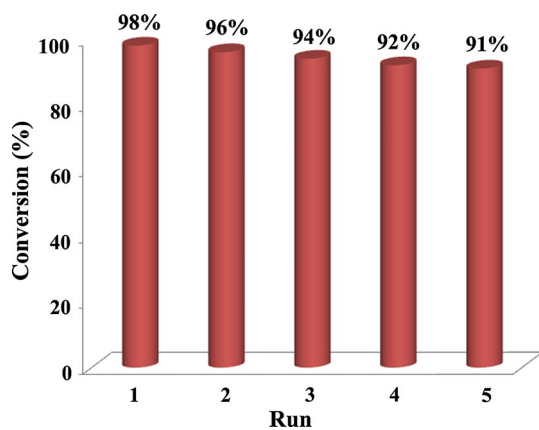
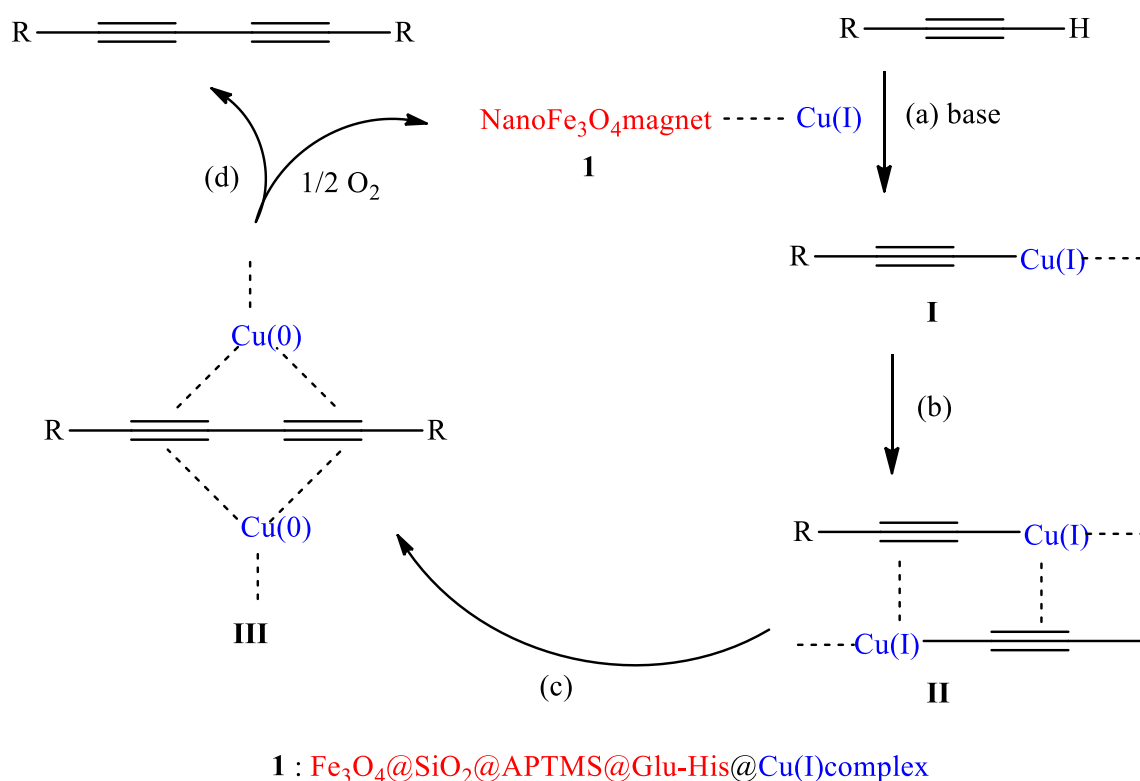


Fig. 12 The effect of recyclability of the catalyst $\text{Fe}_3\text{O}_4@\text{SiO}_2@\text{APTMS}@$ Glu-His@Cu complex for the homocoupling reaction of phenylacetylene at optimum condition

Conclusions

$\text{Fe}_3\text{O}_4@\text{SiO}_2@\text{APTMS}@$ Glu-His@Cu complex (**1**) was prepared from modification of iron oxide nanomagnet particles followed by immobilization of glutaraldehyde-histidine Schiff base ligand and then complexation with Cu(I) salt. Compound **1** was found to successfully catalyze the oxidative homocoupling of phenylacetylene, 4-tert-butylphenylacetylene, 4-fluorophenylacetylene and pent-1-yn-3-ol with 98–100 % conversion and 97–100 % selectivity within 60 min. Recovery of the catalyst was easily achieved simply by magnetic decantation using an external magnet. It was also found that the catalyst can be used three times without significant catalytic activity losing. Utilization of magnetic nanoparticle catalyst with promising advantages in comparison to those of conventional catalyst supports is recommended to be considered by chemical industry researchers.



Scheme 2 Suggested mechanism for the C–C homocoupling of terminal alkynes using compound **1** as catalyst (reaction condition: solvent: benzonitrile at 100 °C, under O_2 atmosphere)

Acknowledgments The financial support from Alzahra University is gratefully acknowledged.

References

- P. Siemsen, R.C. Livingston, F. Diederich, *Angew. Chem. Int. Ed.* **39**, 2632 (2000)
- A.L.K. Shi-Shun, R.R. Tykwinski, *Angew. Chem. Int. Ed.* **45**, 1034 (2006)
- Y.Z. Zhuo, H.Y. Ma, H. Chen, L. Qiao, Y. Yao, J.Q. Cao, Y.H. Pei, *Chem. Pharm. Bull.* **54**, 1455 (2006)
- D. Lechner, M. Stavri, M. Oluwatuyi, R. Pereda-Miranda, S. Gibbons, *Phytochemistry* **65**, 331 (2004)
- L. Hansen, P.M. Boll, *Phytochemistry* **25**, 285 (1986)
- H. Matsunaga, M. Katano, H. Yamamoto, H. Fujito, M. Mori, K. Takata, *Chem. Pharm. Bull.* **38**, 3480 (1990)
- Y.L. Li, J. Li, N.L. Wang, X.S. Yao, *Molecules* **13**, 1931 (2008)
- K. Balaraman, V. Kesavan, *Synthesis* **20**, 3461 (2010)
- T.R. Hoye, P.R. Hanson, *Tetrahedron Lett.* **34**, 5043 (1993)
- R.E. Martin, F. Diederich, *Angew. Chem. Int. Ed.* **38**, 1350 (1999)
- M.M. Haley, *Pure Appl. Chem.* **80**, 519–532 (2008)
- K. Yin, C.J. Li, J. Li, X.S. Jia, *Appl. Organomet. Chem.* **25**, 16 (2011)
- X. Niu, C. Li, J. Li, X. Jia, *Tetrahedron Lett.* **53**, 5559 (2012)
- F. Alonso, T. Melkonian, Y. Moglie, M. Yus, *Eur. J. Org. Chem.* **2011**, 2524 (2011)
- C. Glaser, *Ber. Dtsch. Chem. Ges.* **2**, 422 (1869)
- W.S. Zhang, W.J. Xu, F. Zhang, G.R. Qu, *Chin. Chem. Lett.* **24**, 407 (2013)
- L. Li, J. Wang, G. Zhang, Q. Liu, *Tetrahedron Lett.* **50**, 4033 (2009)
- Y. Kim, A. Park, K. Park, S. Lee, *Tetrahedron Lett.* **52**, 1766 (2011)
- Q. Zheng, R. Hua, Y. Wan, *Appl. Organomet. Chem.* **24**, 314 (2010)
- M. Yu, D. Pan, W. Jia, W. Chen, N. Jiao, *Tetrahedron Lett.* **51**, 1287 (2010)
- F.V. Singh, M.F.Z.J. Amaral, H.A. Stefani, *Tetrahedron Lett.* **50**, 2636 (2009)
- F. Nador, M.A. Volpe, F. Alonso, A. Feldhoff, A. Kirschning, G. Radivoy, *Appl. Catal. A* **455**, 39 (2013)
- J.P. Wan, S. Cao, Y. Jing, *Appl. Organomet. Chem.* **28**, 631 (2014)
- G. Cheng, H. Zhang, X. Cui, *RSC Adv.* **4**, 1849 (2014)
- X. Meng, C. Li, B. Han, T. Wang, B. Chen, *Tetrahedron* **66**, 4029 (2010)
- R. Xiao, R. Yao, M. Cai, *Eur. J. Org. Chem.* **2012**, 4178 (2012)
- P. Kuhn, A. Alix, M. Kumarraja, B. Louis, P. Pale, J. Sommer, *Eur. J. Org. Chem.* **2009**, 423 (2009)
- T. Oishi, T. Katayama, K. Yamaguchi, N. Mizuno, *Chem. Eur. J.* **15**, 7539 (2009)
- K. Yamaguchi, T. Oishi, T. Katayama, N. Mizuno, *Chem. Eur. J.* **15**, 10464 (2009)
- Z. Ma, X. Wang, S. Wei, H. Yang, F. Zhang, P. Wang, M. Xie, J. Ma, *Catal. Commun.* **39**, 24 (2013)
- S. Tang, L. Wang, Y. Zhang, S. Li, S. Tian, B. Wang, *Fuel Process. Technol.* **95**, 84 (2012)

32. J.J. Martínez, H. Rojas, L. Vargas, C. Parra, M.H. Brijaldo, F.B. Passos, J. Mol. Catal. A: Chem. **383–384**, 31 (2014)
33. S.J. Hoseini, V. Heidari, H. Nasrabadi, Mol. Catal. A: Chem. **396**, 90 (2015)
34. S.W. Chen, Z.C. Zhang, M. Ma, C.M. Zhong, S.G. Lee, Org. Lett. **16**, 4969–4971 (2014)
35. Q. Zhu, S. Maeno, M. Sasaki, T. Miyamoto, M. Fukushima, Appl. Catal. B: Environ. **163**, 459 (2015)
36. F. Farzaneh, Z. Shafie, E. Rashtizadeh, M. Ghandi, React. Kinet. Mech. Catl. **110**, 119 (2015)
37. X. Liu, Z. Ma, J. Xing, H. Liu, J. Magn. Magn. Mater. **270**, 1 (2004)
38. P.C. Sahoo, Y.N. Jang, S.W. Lee, J. Mol. Catal. B Enzym. **82**, 37 (2012)
39. W. Wu, Q. He, C. Jiang, Nanoscale Res. Lett. **3**, 397 (2008)
40. D.T. Tran, C.L. Chen, J.S. Chang, J. Biotechnol. **158**, 112 (2012)
41. A. Bagheri, M. Taghizadeh, M. Behbahani, A.A. Asgharinezhad, M. Salarian, A. Dehghani, H. Ebrahimzadeh, M.M. Amini, Talanta **99**, 132 (2012)
42. N. Mizuno, K. Kamata, Y. Nakagawa, T. Oishi, K. Yamaguchi, Catal. Today **157**, 359 (2010)